Cell Reports
Physical Science

Article

Process intensification for the biological production of the fuel precursor butyric acid from biomass

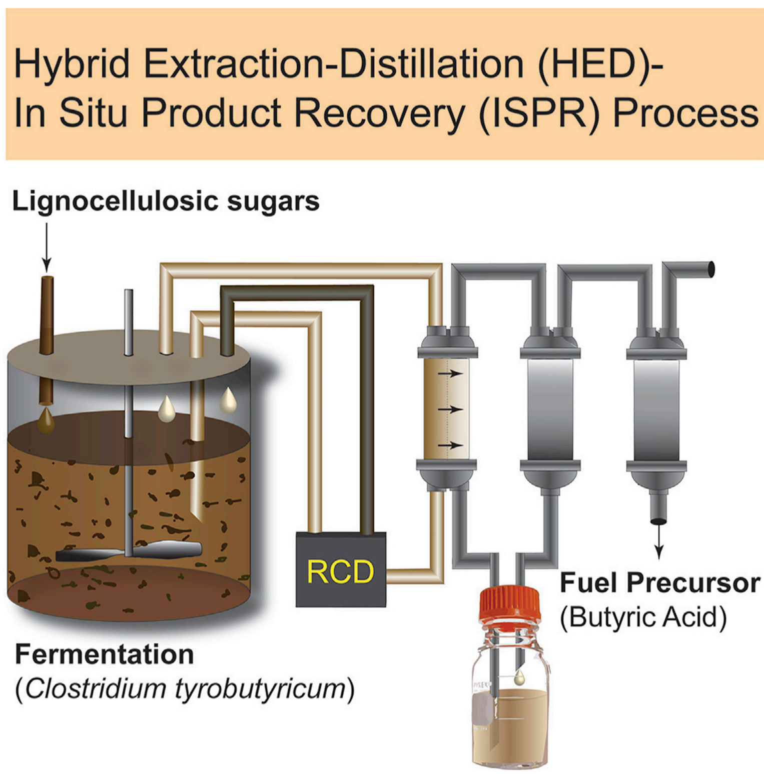

Salvachúa et al. present the development of a fully integrated process to produce a fuel precursor, butyric acid, from lignocellulosic sugars and show that the selling price of butyric acid is significantly lower than that of petroleum. The study includes anaerobic fermentation, bioprocess development, separations science, and economic and environmental assessments.

Davinia Salvachúa, Patrick O. Saboe, Robert S. Nelson, ..., Gregg T. Beckham, Eric M. Karp, Jeffrey G. Linger

davinia.salvachua@nrel.gov (D.S.)
eric.karp@nrel.gov (E.M.K.)
jeffrey.linger@nrel.gov (J.G.L.)

Highlights

Butyric acid is a promising bio-based precursor for diesel and jet fuel

An integrated, energy-efficient process for butyrate production is developed

Neat butyrate is recovered via hybrid extraction-distillation (HED)-ISPR processes

Techno-economic and life cycle assessment favor HED-ISPR processes

Salvachúa et al., Cell Reports Physical Science *2*, 100587
October 20, 2021
https://doi.org/10.1016/j.xcrp.2021.100587

Cell Reports
Physical Science

CellPress
OPEN ACCESS

Article

Process intensification for the biological production of the fuel precursor butyric acid from biomass

Davinia Salvachúa,[1,4,5,*] Patrick O. Saboe,[1,4] Robert S. Nelson,[2] Christine Singer,[1] Ian McNamara,[3] Carlos del Cerro,[1] Yat-Chen Chou,[2] Ali Mohagheghi,[2] Darren J. Peterson,[1] Stefan Haugen,[1] Nicholas S. Cleveland,[1] Hanna R. Monroe,[1] Michael T. Guarnieri,[2] Eric C.D. Tan,[3] Gregg T. Beckham,[1] Eric M. Karp,[1,*] and Jeffrey G. Linger[1,*]

SUMMARY

The production of fuels from lignocellulosic biomass is key to reduce our reliance on petroleum and to promote a sustainable bioeconomy. Butyric acid (BA) is a promising chemical precursor for the production of renewable diesel and jet fuels. BA can be biologically produced from lignocellulosic sugars. However, challenges associated with product selectivity and recovery must be overcome to achieve industrially relevant metrics. Here, we evaluate various fermentation configurations and demonstrate near-homo-butyrate production by using the biocatalyst *Clostridium tyrobutyricum*. We also develop an advanced *in situ* product recovery process based on hybrid extraction-distillation (HED-ISPR) and conduct techno-economic analyses and life cycle assessments. We demonstrate that the HED-ISPR process lowers the overall capital and operating expenses and environmental impact compared to other traditional fermentation processes. Overall, BA minimum product selling price from biomass is 55% of the current BA selling price from petroleum, a significant decrease toward viable renewable fuel production.

INTRODUCTION

The production of biofuels from lignocellulosic resources is key to the realization of a bioeconomy.[1,2] However, the development of technologies for efficient lignocellulose conversion and the search for new molecules with adequate combustion and/or performance-advantaged properties are still required to compete with petroleum-based fuels.[3,4] Recently, butyric acid (BA) has been realized as a promising fuel precursor for the production of renewable diesel and aviation fuels.[5–9] Currently, BA is produced mainly from the oxidation of butyraldehyde obtained from the oxo synthesis of petroleum-derived propylene and used for the production of thermoplastic cellulose acetate butyrate, with a global market of ~80,000 tons/year at a price of ~\$1.8/kg.[10] Therefore, finding sustainable processes for BA production is also a promising path for chemical markets.

Short-chain fatty acids, among them BA, can be produced via anaerobic fermentation from lignocellulose.[11] BA is produced by a large variety of bacteria,[10,12] but very few have been studied for industrial applications. Among them, *Clostridium tyrobutyricum* and *C. butyricum* have received increased attention.[10,13] These bacteria are able to ferment the two primary lignocellulosic sugars, glucose and xylose, and generate butyrate, acetate, CO_2, and H_2 as major products.[14] However, knowledge surrounding these

[1]Renewable Resources and Enabling Sciences Center, National Renewable Energy Laboratory, Golden, CO 80401, USA

[2]Biosciences Center, National Renewable Energy Laboratory, Golden, CO 80401, USA

[3]Catalytic Carbon Transformation and Scale-up Center, National Renewable Energy Laboratory, Golden, CO 80401, USA

[4]These authors contributed equally

[5]Lead contact

*Correspondence:
davinia.salvachua@nrel.gov (D.S.),
eric.karp@nrel.gov (E.M.K.),
jeffrey.linger@nrel.gov (J.G.L.)

https://doi.org/10.1016/j.xcrp.2021.100587

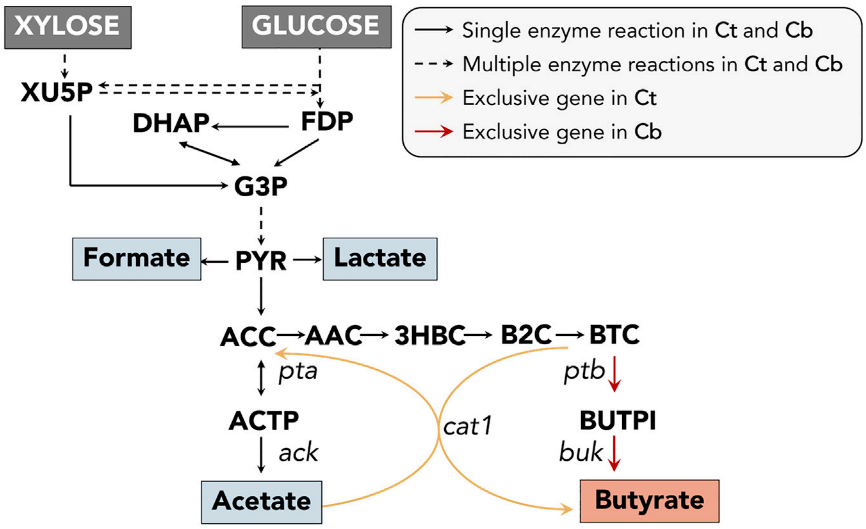

Figure 1. Simplified metabolic map for BA production in *C. butyricum* (Cb) and *C. tyrobutyricum* (Ct)
The map highlights genes for the production of BA in the different *Clostridia* strains and potential by-products (blue squares). Gene abbreviations: *ack*, acetate kinase; *buk*, butyrate kinase; *cat1*, acetoacetyl-CoA transferase; *pta*, phosphotransacetylase; *ptb*, phosphotransbutyrylase. Metabolite abbreviations: 3HBC, (S)-3-hydroxybutanoyl-CoA; AAC, acetoacetyl-CoA; ACC, acetyl-CoA; ACTP, acetyl phosphate; B2C, crotonyl-CoA; BTC, butyryl-CoA; BUTPI, butyryl phosphate; DHAP, bdhydroxyacetone phosphate; FDP, D-fructose 1,6-bisphosphate; G3P, glyceraldehyde 3-phosphate; PYR, pyruvate; XU5P, D-xylulose 5-phosphate.

microbes' glucose and xylose co-utilization capabilities and the production of minor products (i.e., formate and lactate[8,14,15]) is scarce. From a metabolic point of view, *C. tyrobutyricum* has been recently reported to produce BA only via a transferase reaction (which converts butyryl-coenzyme A [CoA] to BA through acetate reassimilation),[15] and not via *ptb/buk* genes (which convert butyryl-CoA to butyryl-phosphate and BA[10]), as previously assumed,[16–18] and as reported for *C. butyricum*[13] (Figure 1). These metabolic disparities may lead to substantially different product selectivity results, which warrant further analyses in industrially relevant cultivation conditions.

Similar to other acidogenic bacteria, *C. tyrobutyricum* and *C. butyricum* are strongly inhibited by their acidic products. BA toxicity involves cell membrane damage, disruption of the transmembrane pH gradient, and reduction of ATP levels, which are exacerbated at lower pHs.[19] Continuous fermentation configurations can alleviate this toxicity by constantly flowing cultivation media through the bioreactors.[20,21] However, this fermentation strategy typically leads to low product titers and requires acid neutralization in the bioreactor, which increases process costs.[22] An alternative route to decrease product toxicity is via *in situ* product recovery (ISPR) processes. Liquid-liquid extraction (LLE) is commonly used in ISPR processes to extract short-chain fatty acids from bioreactors into organic solvents, which reduces their concentration in the bioreactor and effectively prevents product inhibition.[23–26] The acid product is then recovered from the organic solvent via back-stripping into a base (e.g., NaOH).[26] This process is not practical on the industrial scale because the LLE-ISPR processes have a significant base cost and a large associated environmental impact.[22,27] Therefore, advanced ISPR processes that do not require significant base loads are sought. To that end, a hybrid extraction-distillation (HED)-ISPR process was recently proposed for the recovery of carboxylic acids from simulated fermentation broth,[22] which differs from traditional LLE-ISPR processes by selectively recovering purified BA from the organic extract with distillation rather than back-stripping into alkaline solutions. HED-ISPR processes have also been successfully utilized for other applications such as the recovery of ethyl esters from mock mixtures.[28] However, to our knowledge, HED-ISPR processes have not yet been integrated with biological systems, which is needed to validate the process and identify potential bacterial and separation performance issues.

ISPR processes for the production of biofuel precursors face challenges that include (1) minimizing the energy consumption to less than the product's higher heating value (HHV)[29] to achieve sustainable processing and (2) maintaining system sterility by separating cellular debris from the fermentation broth before molecular separation units.[30] Our previous work[22] highlighted that lowering the bioreactor pH and selecting an effective extractant are two key process design components that may lead to a HED-ISPR energy demand below ~20% of the BA HHV. An example of a strong extractant is phosphine oxide-based extractant, which efficiently extracts free (protonated) BA at pHs $\leq$ 5[22] by forming an acid-base pair with the acidic proton on BA. To address maintaining sterility and to prevent long-term fouling of the HED-ISPR equipment, a rotating ceramic disk (RCD) microfiltration module may be coupled to an external fermentation loop. Dynamic filtration systems, such as the RCD, are robust cell- and debris-retention devices because they allow long system uptimes before a cleaning cycle is needed, and require low pumping energy compared to traditional cross-flow systems.[30–32]

In this work, we compare the performance of *C. tyrobutyricum* and *C. butyricum* side by side at diverse pHs in batch fermentation mode. *C. tyrobutyricum* achieved considerably higher BA selectivities from mixed sugars than *C. butyricum*. Thus, *C. tyrobutyricum* was selected for further metabolic analyses and process development at low pHs (pH ~5) in different fermentation setups (i.e., batch, fed-batch [FB], LLE-ISPR, and HED-ISPR coupled to a RCD) with corn stover hydrolysate. Based on the fermentation data and BA downstream recovery from this study, techno-ecomomic analysis (TEA) and life cycle assessments (LCA) were conducted and revealed that BA production via the HED-ISPR process results in dramatically favorable economics and reduced environmental effects (i.e., greenhouse gas [GHG] emissions and fossil energy demand [FED]) compared to other fermentations setups. Overall, HED-ISPR performance, TEA, and LCA show a promising path for lignocellulose conversion to BA for use as a chemical intermediate for the production of renewable fuels.

RESULTS

BA selectivity is significantly higher in *C. tyrobutyricum* than *C. butyricum*

Fermentation and LLE-ISPR performance are both typically highly sensitive to small changes in pH. While *C. tyrobutyricum* and *C. butyricum* grow better at near-neutral pHs,[10,24,33] low pH operation is critical for efficient extraction of BA in a LLE-ISPR setting.[22] Therefore, we compared the performance of these bacteria at pH 5, 5.5, 6, and 7 while fermenting mock corn stover hydrolysate in batch mode. The mock hydrolysate mimics the sugar concentration ratios in corn stover hydrolysate (30 g/L glucose, 15 g/L xylose, 5 g/L arabinose, and 2 g/L galactose) (Table S1). To facilitate the visualization of Figure 2, the bacterial performance at pH 7 only is shown in Figures S1–S3. *C. butyricum* co- utilized both sugars at all the pHs tested (Figures 2A and S1A–S1D). At pH 5, neither glucose nor xylose were fully consumed, which can be attributed to the higher toxicity of the pool of acid products at the lower pHs.[19] In contrast, *C. tyrobutyricum* showed a diauxic behavior in which xylose was utilized only after glucose was depleted from the media (Figure 2B). We observed this behavior at pH 6 and pH 7 since xylose utilization was negligible at pH 5.5 and pH 5 (Figures 2B and S1I–S1L). Glucose was fully utilized by *C. tyrobutyricum* at pH 5

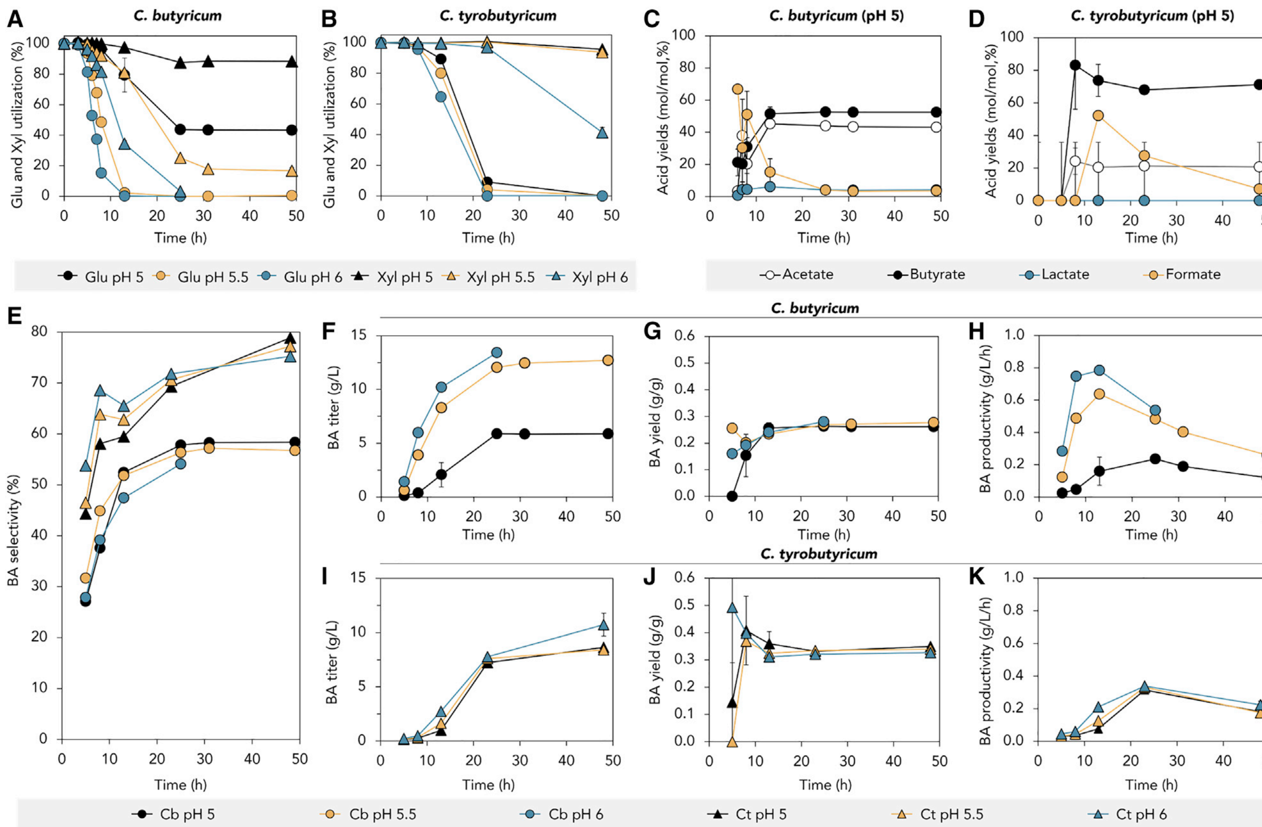

Figure 2. Metabolic and process parameters from batch fermentations conducted with wild-type *C. butyricum* and *C. tyrobutyricum* on mock corn stover hydrolysate at an initial sugar concentration of 50 g/L

(A and B) Glucose (Glu) and xylose (Xyl) utilization (%) at pH 5, 5.5, and 6 in (A) *C. butyricum* and (B) *C. tyrobutyricum*. A value of 100% corresponds to the initial glucose (~30 g/L) or xylose (~15 g/L) concentration.

(C and D) Metabolic yields for BA, acetate, lactate, and formate at pH 5 in (C) *C. butyricum* and (D) *C. tyrobutyricum*.

(E) BA selectivity at pH 5, 5.5, and 6 in *C. butyricum* (Cb) and *C. tyrobutyricum* (Ct).

(F–K) Process parameters. (F and I) BA titers, (G and J) BA process yields, and (H and K) BA productivities in (F)–(H) *C. butyricum* and (I)–(K). *C. tyrobutyricum* at pH 5, 5.5, and 6.

Results show the average of biological duplicates. Error bars show the absolute difference between biological duplicates.

Additional fermentation profiles are shown in Figures S1, S2, and S3.

and showed a higher maximum instantaneous utilization rate (2.0 g/L/h) than that observed for *C. butyricum* at the same pH. Regarding minor sugars, *C. butyricum* utilized galactose at every pH, while arabinose was utilized only at pH 7 (Figures S1A–S1D). In contrast, galactose and arabinose utilization was not appreciable in any case in *C. tyrobutyricum* (Figures S1I–S1L). These results show that *C. butyricum* is, in general, a more efficient bacterium than *C. tyrobutyricum* for sugar co-utilization.

Metabolic yields for BA and other by-products were strain and pH dependent (see Note S1, Figures 2C, 2D, S3D–S3F, and S4) but, in general, BA metabolic yields were higher in *C. tyrobutyricum* than in *C. butyricum*. BA selectivity (calculated as BA [g/L] divided by total acids [g/L], including BA, acetate, lactate, and formate) was also considerably higher in *C. tyrobutyricum* than in *C. butyricum* at pH 5, as well as BA titers, process yields, and overall productivities (Figures 2E–2K). Despite these results, we sought to engineer *C. butyricum*, due to its greater efficiency co-using sugars, to increase flux to BA (seeFigure S5–S7; Table S2; Note S2). However, BA metabolic yields still remained lower than those observed in *C. tyrobutyricum*. Therefore, we selected *C. tyrobutyricum* for further process development and metabolic studies.

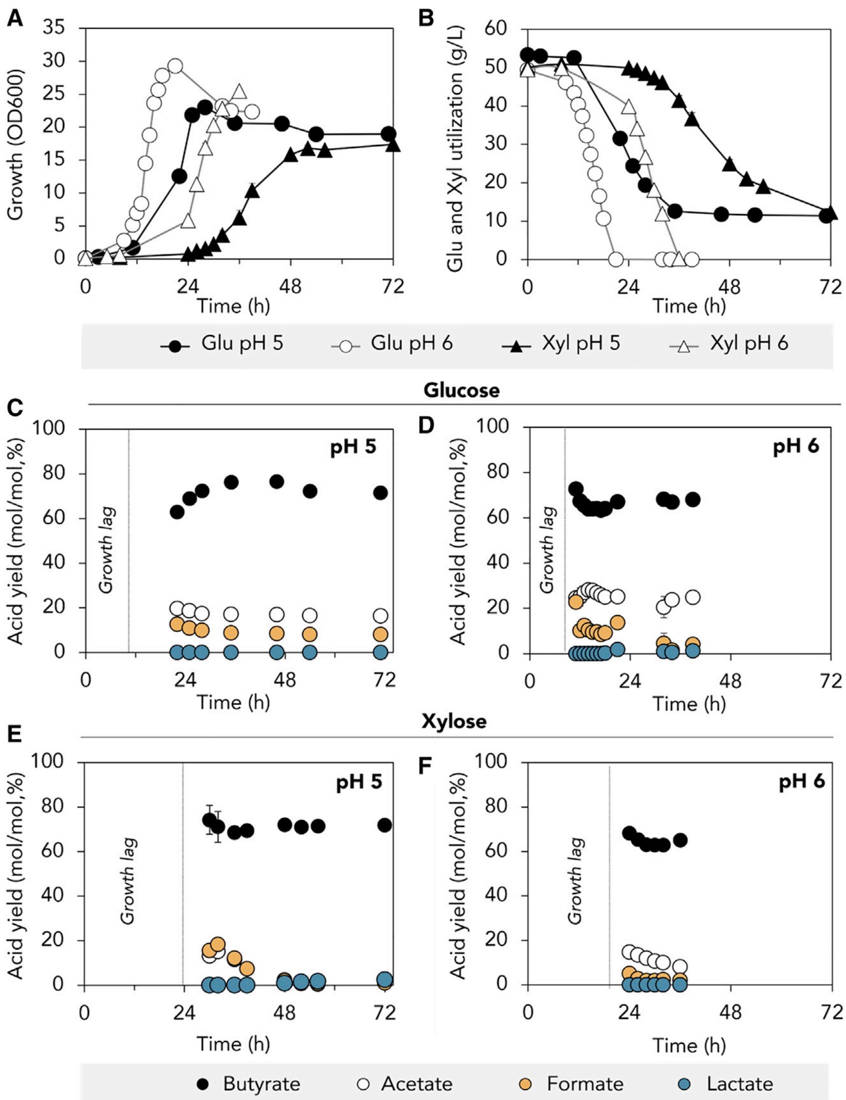

Figure 3. Performance of *C. tyrobutyricum* in batch fermentations containing glucose and xylose as the sole carbon sources at pH 5 and pH 6

(A) Bacterial growth (OD 600).

(B) Glucose and xylose utilization at pH 5 and pH 6.

(C and D) Acid metabolic yields in glucose containing fermentations at pH 5 and pH 6.

(E and F) Acid metabolic yields in xylose containing fermentations at pH 5 and pH 6.

Results show the average of biological duplicates. Error bars show the absolute difference between biological duplicates.

Xylose is catabolized at pH 5 by *C. tyrobutyricum*

The conversion of xylose is necessary for the economical valorization of lignocellulose. As shown above (Figure 2B), xylose utilization by *C. tyrobutyricum* was negligible at pH 5 and pH 5.5 in mock hydrolysates. Therefore, we sought to understand whether inefficient xylose utilization was solely the result of low pH or catabolite repression due to the presence of glucose. For this purpose, we evaluated the performance of *C. tyrobutyricum* in medium containing either xylose (50 g/L) or glucose (50 g/L) as the sole carbon sources at pH 5 and 6 (Figures 3A, 3B, and S8) and compared it with the previous results in mock hydrolysate. *C. tyrobutyricum* grew in all cases; however, the initial growth lags were considerably longer on xylose than glucose (Figures 3A and S8). The maximum sugar utilization rates also decreased at the lower pHs from 5.2 to 2.4 g (glucose)/L/h and from 4 to 1.3 g (xylose)/L/h at pH 6 and 5, respectively. These results validate that xylose can be utilized by *C. tyrobutyricum* at pH 5 as the sole carbon source (Figure 3B) (which is consistent with previous literature[18]) and that the presence of glucose (Figure 2B) is responsible for the inefficient xylose utilization at pH 5. Interestingly, regarding metabolic yields, there were important differences, depending on the carbon source (Figures 3C–3E). Specifically, acetate yields were relatively constant in glucose but decreased down to zero in xylose at pH 5 (time at which lactate was also produced). Because these fermentations suffer from product toxicity, especially those conducted at pH 5, ISPR will be an important process to help fully understand metabolic differences and trends among different media.

Sugar co-utilization was promoted in FB fermentations on corn stover hydrolysate by *C. tyrobutyricum*

Considering that xylose can be utilized at pH 5 by *C. tyrobutyricum*, we aimed to enhance glucose and xylose co-utilization capabilities. For that purpose, we developed a seed culture containing *C. tyrobutyricum* actively utilizing xylose (hereafter, induced seed) (see Figures S9–S11; Note S3) and compared sugar co-utilization from both induced and non-induced seeds in more relevant process conditions (on corn stover hydrolysate [Table S1] at pH 5, at an initial xylose concentration of 25 g/L, and in FB mode [Figure 4A]). *C. tyrobutyricum* utilized a final xylose concentration of 5 and 2.3 g/L when inoculated from induced and non-induced seeds, respectively (Figures 4A and S12). However, because sugar utilization terminated early (<40 h, mainly due to toxicity to products), we cannot prove considerable co-utilization improvements based on seed origin. Thus, before shifting to LLE-ISPR processes, we conducted the same experiment at pH 6. In addition, we also included (1) batch fermentations from both induced and non-induced seeds (Figures 4B and S13) and (2) batch and FB fermentations at an initial sugar concentration of 50 g/L from both induced and non-induced seeds (Figures 4C and S14). To test reproducibility, we also conducted two independent experiments (each with biological duplicates), for the FB cultivation cases from induced seed cultures. Xylose utilization was improved in batch fermentations when using the induced seed culture at an initial sugar concentration of 25 and 50 g/L (Figures 4B and 4C). However, in FB mode, the effect of the induction was less evident, and sugars were co-utilized in all cases (Figures 4B and 4C). In cultivations containing an initial sugar concentration of 50 g/L from induced seed cultures, xylose utilization rates were considerably improved in FB mode compared to batch mode. Overall, these observations suggest that although induced seed cultures may promote an initial higher xylose utilization rate, a FB fermentation strategy (Figures S13 and S14) is more critical to enhance xylose utilization in *C. tyrobutyricum* under the conditions investigated here (Figure 4C). Concerning BA titers, yields, and productivities (Figures 4D–4F), the FB strategy at an initial sugar concentration of 50 g/L showed the best results compared to the other conditions due to the lower generation of by-products (specifically lactate, see Note S4) and higher BA metabolic yields (Figure S15).

C. tyrobutyricum fermentations in LLE-ISPR processes with acids recovery in NaOH enhances BA production and provides metabolic insights

To better understand *C. tyrobutyricum* metabolism at low pHs ($\leq$5), and in an attempt to generate industrially relevant BA titers, yields, and productivities,[34] we employed an LLE-ISPR process. Based on BA inhibition levels and BA productivity results at pHs $\leq$5 (Figures S16 and S17), we selected pH 5 to conduct these fermentations (see Note S5). Note that *C. tyrobutyricum* is only able to produce a maximum BA concentration of $\sim$15 g/L at pH 5 in the standard FB configuration (Figures 4D, 5A, and S8). The LLE-ISPR process (Figure 5B) included 3 external

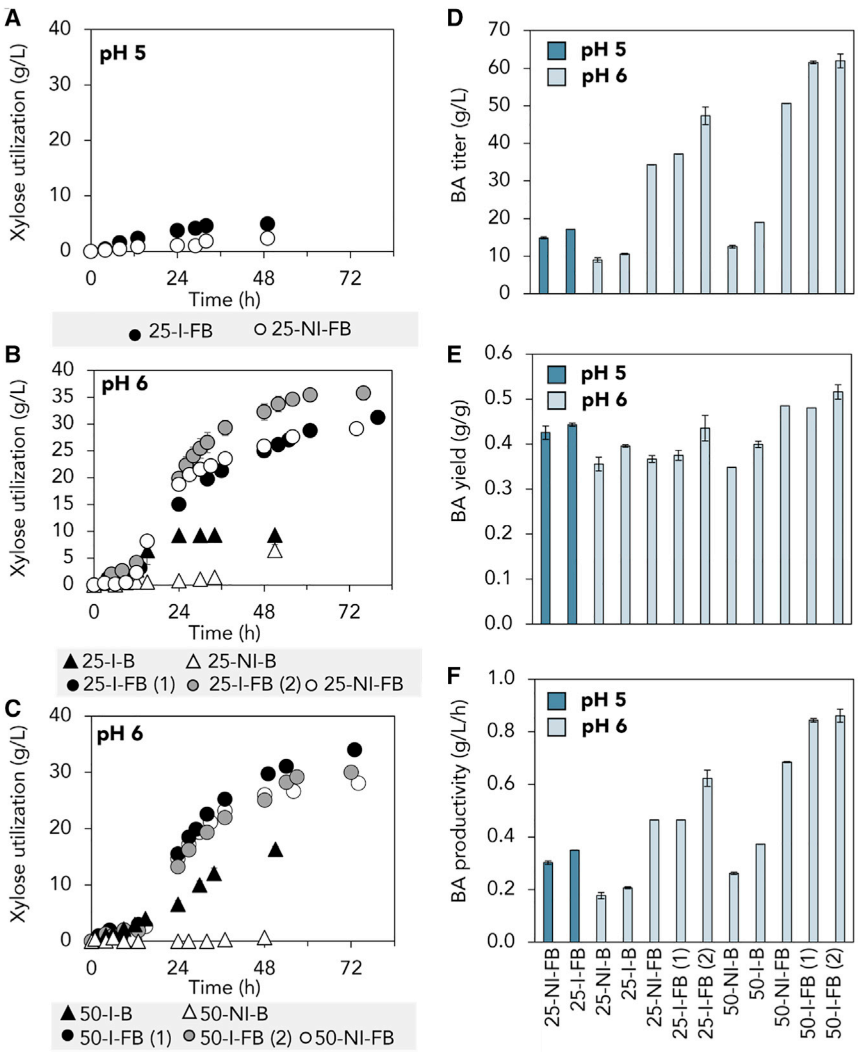

Figure 4. Performance of *C. tyrobutyricum* in batch and fed-batch fermentations containing corn stover hydrolysate

(A) Fed-batch (FB) fermentations from induced (I) and non-induced (NI) seed cultures at pH 5 and at an initial sugar concentration of 25 g/L (25).

(B) Batch (B) and FB fermentations from I and NI seed cultures at pH 6 and at an initial sugar concentration of 25.

(C) B and FB fermentations from I and NI seed cultures at pH 6 and at an initial sugar concentration of 50 g/L (50).

(D) BA titers.

(E) BA process yields.

(F) BA productivities.

Results show the average of biological duplicates. Error bars show the absolute difference between biological duplicates. (1) and (2) represent 2 individual experiments in the same conditions, each including biological duplicates.

Note that all of the fermentations were conducted with Hydrolysate 1, excluding 50-I-FB, which was conducted with Hydrolysate 2 (see Table S1).

process streams: (1) an external fermentation loop directed to an LLE membrane contactor unit; (2) a solvent loop containing 20% of the extractant, trioctylphosphine oxide (TOPO), with 40% 2-undecanone and 40% mineral oil (this mixture was chosen because it was found to be non-toxic and close to the TOPO solubility,

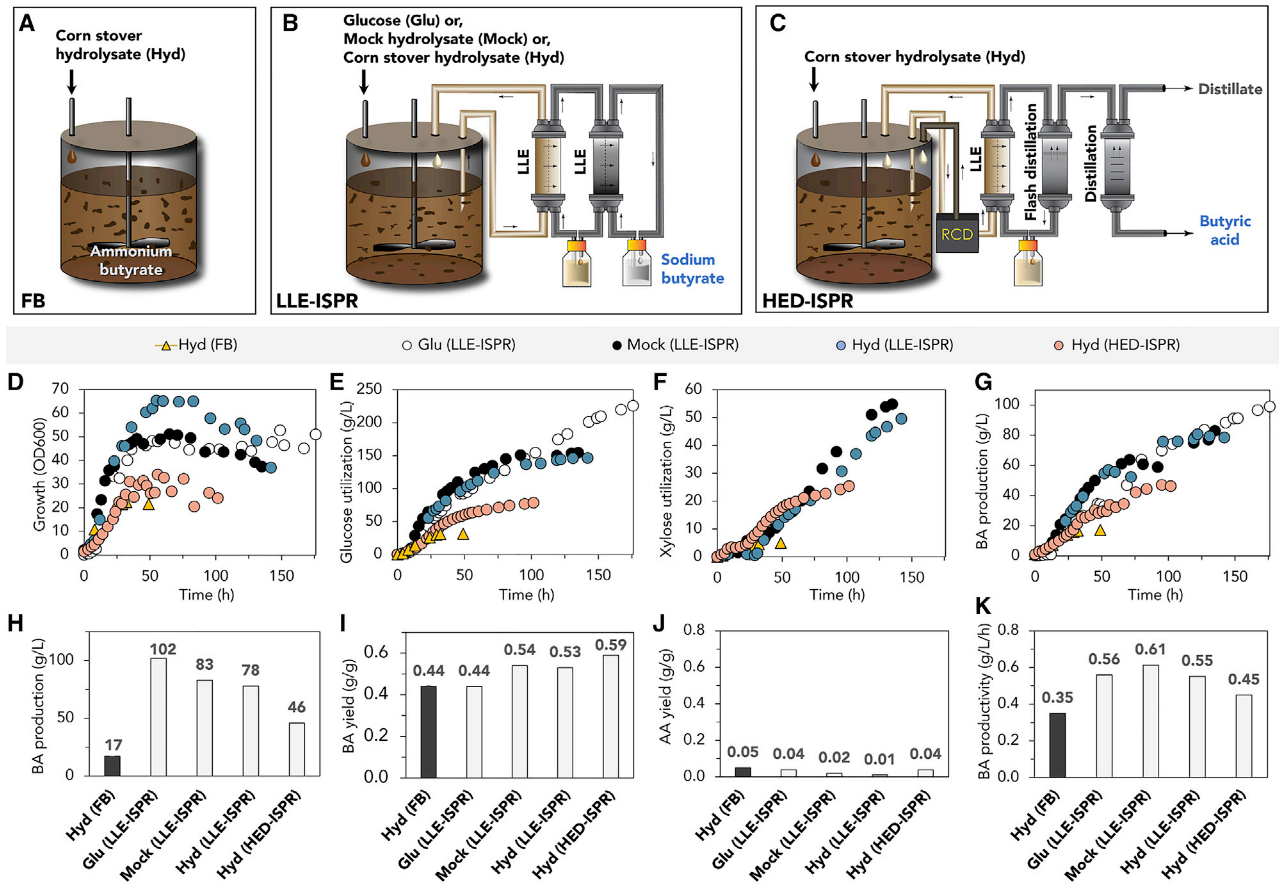

Figure 5. Performance of *C. tyrobutyricum* at pH 5 in various fermentation setups

(A) Diagram of a FB fermentation without acids extraction.

(B) Diagram of an LLE-ISPR process that includes acids recovery in NaOH.

(C) Diagram of an HED-ISPR process that includes cell recycling via a rotary ceramic disk (RCD) and acids recovery in organic solvent and BA recovery via distillation.

(D–K) Fermentation parameters from different setups (FB, LLE-ISPR, HED-ISPR) and carbon sources (corn stover hydrolysate [Hyd], glucose, and mock corn stover hydrolysate [mock]). The parameters depicted are (D) bacterial growth (OD 600), (E) total glucose utilized normalized by the reactor volume (g/L), (F) total xylose utilized normalized by the reactor volume (g/L), (G) total BA in the system normalized by the reactor volume (g/L), (H) total BA produced (g/L), (I) BA yield (g/g), (J) acetate yield (g/g), and (K) overall BA productivity (g/L/h).

For comparison purposes, the results from Hyd (FB) are shown and correspond to the fermentations depicted in Figures 4 and S12A at pH 5 from seeds with induced cells.

thereby promoting extraction); and (3) a back extraction loop, which recirculates a NaOH solution (Figure 5B).

The bioreactors contained three different carbon sources: (1) pure glucose, (2) mock corn stover hydrolysate, or (3) corn stover hydrolysate (hereafter referred to as glucose, mock, and hydrolysate media, respectively) (Figures S18 and 19) and were inoculated with induced cells. The feeding with concentrated sugar solutions was initiated at 12 h. Fermentations were concluded when sugar utilization rates were negligible, or when the bioreactor reached maximum working volumes (the latter case only occurred in glucose media). *C. tyrobutyricum* reached an optical density at 600 nm (OD 600) of 50 in glucose and mock media and 65 in hydrolysate (Figure 5D). Glucose utilization profiles were similar in the different media, and xylose was co-utilized in all cases (Figures 5E and 5F). Arabinose (a minor sugar in corn stover hydrolysate; Table S1) accumulated up to 10 g/L in the bioreactor (Figures S19 and S20). Concerning acid levels inside the bioreactor, BA accumulated to a maximum concentration of 6–7 g/L. Acetate, formate, and lactate remained relatively constant in glucose medium at concentrations lower than 4 g/L. In contrast, acetate and formate were almost fully depleted in mock and hydrolysate media at the end of the cultivations (Figure S19). The low BA levels in the bioreactors validate the efficiency of the LLE-ISPR process. BA extraction was >92% from the total BA produced in each fermentation (Figure S21). In the case of acetate, 64% was extracted from fermentations on glucose medium and >75% from mock and hydrolysate media. Remarkably, the absolute amount of acetate in the whole system (g) decreased almost 2-fold (from its maximum peak at 30–40 h) in mock and hydrolysate media (Figure S21), demonstrating the reassimilation of acetate toward BA (Figure 1). The extraction efficiency can be also demonstrated by examining the pH and base added in the bioreactor. Base (4 N NH_4OH) was only added during the first ~30 h of fermentation to maintain the pH at 5 (Figures S19 and S22).

The amount of BA produced in glucose, mock, and hydrolysate media was 266, 242, and 221 g (Figure S21), respectively (which corresponds to a titer of 102, 83, and 78 g/L, normalized by the final volume in the bioreactor; Figures 5G and 5H). Most important, acetate production was 8.9, 3.4, and 1.9 g/L, respectively, which represents a near-homo-butyrate fermentation. Concerning BA process yields, the highest values were observed in mock and corn stover hydrolysate media, with a concomitant acetate yield of 0.01–0.02 g/g (Figures 5I and 5J). Overall BA productivities were between 0.55 and 0.61 g/L/h (Figure 5K), although productivities as high as 1.1 and 0.8 g/L/h were observed at ~30 h of fermentation in media containing mixed sugars and glucose, respectively (Figure S23). Final C-mol balances were 65%, 55%, and 54% in glucose, mock, and hydrolysate media, respectively (Figure S4) (C-mol balances do not account for cell biomass and CO_2 production; carbon from CO_2 is estimated to be 33% per molecule of glucose[10]).

To understand whether there is any relationship between the termination of the fermentations in the LLE-ISPR processes and *C. tyrobutyricum* metabolism, we analyzed acid metabolic yields over time as well as instantaneous sugar utilization rates (mol/h) between consecutive time points (Figure 6). BA metabolic yields were relatively constant in mock and hydrolysate media (between 75% and 85%) (Figure 6). In glucose medium, BA yields were 65%–75% and increased up to 100% after 75 h (Figure 6), the time at which the cells had already reached the stationary phase (Figure 5D). The flux to other by-products changed significantly over time, especially in mock and hydrolysate media. Specifically, initial acetate and formate metabolic yields were ~20%–30%, but the yields dropped continuously over the fermentation course (close to zero), whereas in glucose medium, acetate yield was maintained at 10% and formate was not detected (Figure 6). The lactate metabolic yield in glucose medium was low but constant between 0.5 and 1.5% after the cells reached the stationary phase. Conversely, lactate was only produced when formate and acetate were near depletion (between 75 and 100 h of cultivation) in mock and hydrolysate media (Figure 6). Interestingly, examining the instantaneous sugar utilization rates, although glucose is preferentially utilized at the beginning of the cultivations in mixed sugars cultivations, the rate decreased and equaled xylose utilization rates at ~100 h (Figure 6). These results suggest the presence of a metabolic shift when xylose is part of the media composition, potentially due to redox or energetic imbalances, which prematurely terminates the fermentations relative to glucose-only-containing cultivations.

Fermentation performance metrics achieved in HED-ISPR processes

We further evaluated BA production by *C. tyrobutyricum* using a HED-ISPR process. There are three main differences in the HED-ISPR process (Figures 5C and S24)

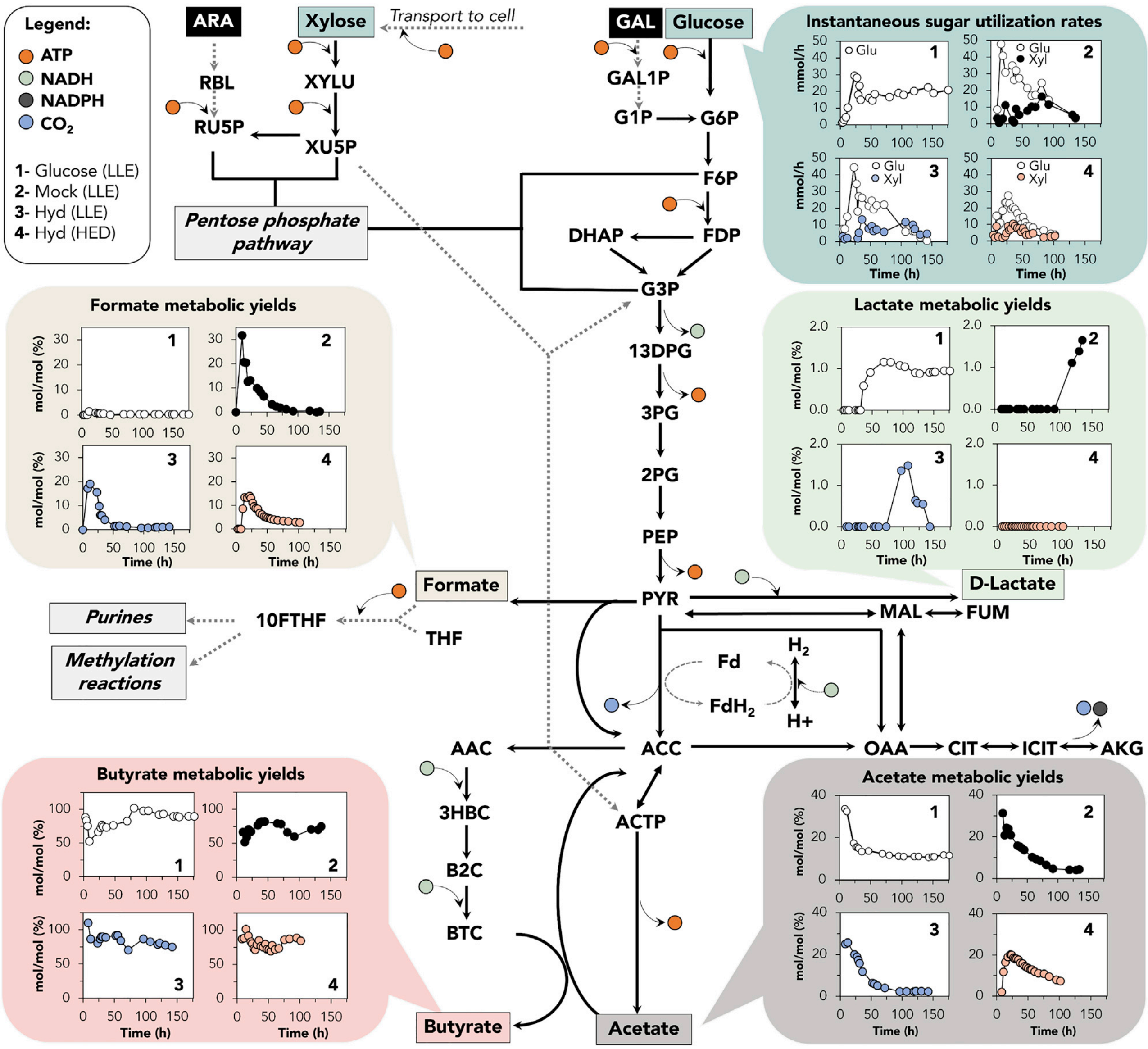

Figure 6. Scheme of *C. tyrobutyricum* central metabolism

The map highlights metabolic yields for the different acid products and instantaneous glucose and xylose utilization rates in different LLE-ISPR setups at pH 5. Metabolic yields (mol acid/mol sugars utilized) are depicted for BA, acetate, formate, and lactate while fermenting (1) glucose in the fermentation setup shown in Figure 5B), (2) mock hydrolysate in the fermentation setup shown in Figure 5B, (3) corn stover hydrolysate in the fermentation setup shown in Figure 5B, and (4) corn stover hydrolysate in the fermentation setup shown in Figure 5C. Discontinuous lines correspond to hypothesized metabolic steps in *C. tyrobutyricum* (non-experimentally confirmed). Metabolite abbreviations: 13DPG, 3-phospho-D-glyceroyl phosphate; 2PG, D-glycerate 2-phosphate; 3HBC, (S)-3-hydroxybutanoyl-CoA; 3PG, 3-phospho-D-glycerate; 10FTHF, 10-formyltetrahydrofolate; AAC, acetoacetyl-CoA; ACC, acetyl-CoA; ACTP, acetyl phosphate; AKG, 2-oxoglutarate; ARA, D-arabinose; B2C, crotonyl-CoA; BTC, butyryl-CoA; BUTPI, butyryl phosphate; CIT, citrate; DHAP, dihydroxyacetone phosphate; FDP, D-fructose 1,6-bisphosphate; F6P, D-fructose 6-phosphate; FUM, fumarate; G1P, D-glucose 1-phosphate; G3P, glyceraldehyde 3-phosphate; G6P, D-glucose 6-phosphate; GAL, D-galactose; GAL1P, alpha-D-Galactose 1-phosphate; ICIT, isocitrate; MAL, malate; OAA, oxaloacetate; PEP, phosphoenolpyruvate; PYR, pyruvate; RBL, D-ribulose; RU5P, D-ribulose 5-phosphate; THF, tetrahydrofolate; XU5P, D-xylulose 5-phosphate; XYLU, D-xylulose.

compared to the traditional LLE-ISPR process (Figure 5B). First, RCD microfiltration is used to remove cells before extraction. Second, the extractant used was 70% Cyanex 923 (a commercially available phosphine oxide extractant) in mineral oil rather than the 20% TOPO + 40% undecanone + 40% mineral oil extractant used in the LLE-ISPR process. The 70% Cyanex 923 was used because it allows a greater concentration of BA in the organic extract, which is important for distillation feasibility (it lowers the volume of loaded extractant sent to the flash column and thus lowers the process energy consumption). Third, the BA is recovered from the organic extract via distillation rather than by back extraction into an NaOH solution. Thus, the BA is recovered as a concentrated free acid, rather than a dilute carboxylate.

Fermentation was conducted in a 2.5-L bioreactor at an initial sugar concentration of 50 g/L from corn stover hydrolysate and the feeding phase was initiated at 12 h (Figures S18 and S19). The growth rate (during the first ~24 h) was slightly lower in this process (HED-ISPR) compared to the LLE-ISPR process (μ = 0.10 and 0.13/h, respectively) (Figure 5D), and there was no evident cell debris in the external RCD loop (Figure S25). Total glucose and xylose utilization at the end of the fermentation was 78 and 25 g/L, respectively (normalized by the reactor volume) (Figures 5E and 5F). The total BA produced was 107 g (or 46 g/L) (Figures 5G and 5H) and the BA yield was higher than that observed in the other fermentations (0.59 g/g) (Figure 5I). The acetic acid (AA) yield was low (0.04 g/g) and the overall BA productivity was 0.45 g/L/h (Figures 5J and 5K), with a maximum productivity peak of 0.71 at 35 h (Figure S23). At the end of the cultivation, 88% of the BA produced was extracted, while 12% remained in the bioreactor loop (<6 g/L) (Figures S19 and S21). In the case of acetate, 43% was extracted, but only 1.6 g/L remained in the bioreactor. The final C-mol balance was 62% (Figure S4) (C-mol balance does not account for cell biomass and CO_2 production). The base addition profile was similar to that in the previous LLE-ISPR processes (up to 30 mL/L, 4 N NH_4O) to maintain the pH at 5, but then the pH was stable from ~40 h to the end of the fermentation without additional base (Figure S22).

At the metabolic level, acids profiles were very similar to those observed in hydrolysate in the LLE-ISPR setup. Acetate and formate yields reduced over time, potentially due to reassimilation. However, in this case, since the fermentations ended earlier (~100 h instead of 150 h; Figure 5), these metabolites were not fully depleted and therefore there was no lactate production. We hypothesized that the fermentations ended earlier in this setup because of a potential toxicity effect of Cyanex 923 in the organic loop. To verify this hypothesis, we evaluated the toxicity of (1) 20% TOPO + 40% undecanone + 40% mineral oil and (2) Cyanex 923. Whereas *C. tyrobutyricum* was able to grow in defined media without solvent and with an overlay of the TOPO-based solvent at a v:v ratio of 100:20, Cyanex 923 containing media at a v:v ratio of 100:0.006 did not allow any growth. Even though the RCD unit prevents cells in the extraction loop, Cyanex 923 has a small solubility in water and likely leads to growth inhibition.

Neat BA recovery

The downstream chemical conversion of BA to renewable fuels and chemicals requires the separation of neat BA from the fermentation broth and the use of the free acid.[8,35] Here, we demonstrate the separation of neat BA from the NaOH loop of the traditional LLE-ISPR process (Figure 5B). We then fully implement the HED-ISPR process using flash and multi-stage distillation to recover neat BA directly from the organic extract (Figure 5C). These separations (see Figures S26–S31; Note S6) were used to guide a comparative TEA and LCA, as detailed in the next section.

TEA and LCA favors the HED-ISPR process

To show the economic differences of the ISPR processes, compared to the conventional FB mode, a comparative TEA was completed for a n^{th}-biorefinery operating in either FB or ISPR mode. The boundary of the TEA within the biorefinery was confined to the fermentation process (FB or ISPR) and the required downstream processing (DSP) to isolate neat BA at the production capacity of ~150 KT/year from 2,000 dry metric tons of biomass per day.[36] The selected production capacity of a nth-biorefinery was previously optimized through economies of scale and transportation cost analysis.[36] Fermentation and DSP capital and operational costs were determined for the three different hydrolysate conversion and separation processes (Figures 5A–5C) to elucidate the cost drivers of BA production in the nth-biorefinery. Specifically, four conversion processes were modeled: (1) FB fermentation operating at pH 5 with post-fermentation DSP (Figure 5A), (2) FB fermentation at pH 6 with post-fermentation DSP (Figure 5A), (3) a LLE-ISPR process operating at pH 5 (Figure 5B), and (4) a HED-ISPR process operating at pH 5 (Figure 5C). Fermentation parameters for each process were modeled by using the experimental data provided above for hydrolysate fermentations for FB (Figure 4) and for ISPR processes (Figures 5H, 5I, and 5K). All of the processes were assumed to operate via a homo-BA fermentation.

The fermentation and DSP capital cost estimates are described below, with the goal to compare equipment costs among the process options. The capital expenditures (CAPEX) was determined assuming that the major equipment have a lifetime equal to the plant lifetime of 30 years. Specific equipment associated with fermentation and DSP is listed in Tables S3–S5. Figure S32 shows the total capital cost as the summation of the major unit operations within each process. Most of the cost of the FB, pH 6 process are associated with the fermentation equipment (54% of total capital) and evaporation equipment (29% of total capital) used in the post-fermentation DSP. For the LLE-ISPR process, the extraction equipment makes up the largest proportion of the capital (50%), followed by the fermentation equipment (39%). The HED-ISPR has a slightly higher capital cost compared to the LLE-ISPR process, partially due to the addition of the dynamic filtration. The dynamic filtration system in the HED-ISPR comprises 28% of the capital cost, following the fermentation equipment capital cost (39%). The total capital cost for each process was then normalized to the total amount of BA produced by the plant to allow comparison of the processes' capital costs in terms of $/BA. The fermentation and DSP capital cost associated with the FB (pH 5), FB (pH 6), LLE-ISPR, and HED-ISPR process is $0.011, $0.007, $0.013, and $0.014/kg BA, respectively (Figure S32).

Fermentation and DSP operating expenses (OPEX) were determined accounting for the raw material cost (Table S6), and utilities cost (Table S7) for each process (additional TEA information for each unit operation is provided in Tables S8–S14). The operating costs associated with fermentation included the nutrient, neutralization source (NH_4OH, to maintain pH), and electricity utility costs. The total fermentation operating cost is shown in Figure S33A. All 4 cases have the same nutrient cost because the ratio between nutrients and feedstock capacity (2,000 dry metric ton of biomass per day) is a constant across the cases. However, the cost of the NH_4OH varies across cases due to differences in the operating pH, fermentation productivity, and mode (FB or ISPR). NH_4OH costs dominate fermentation OPEX: 80%, 89%, 46%, and 57% for the FB (pH 5), FB (pH 6), LLE-ISPR, and HED-ISPR, respectively. The driver of difference between the NH_4OH costs is a result of the differences in pH and productivity. In both ISPR cases, NH_4OH is added to the fermenter in similar amounts during start-up; however, the LLE-ISPR process has a higher productivity than the HED-ISPR process (Figure 5K), and thus more BA is produced per mole of NH_4OH added to the system. The electricity requirement for each process is the energy needed to maintain the pumps and impellers in the fermentation unit.

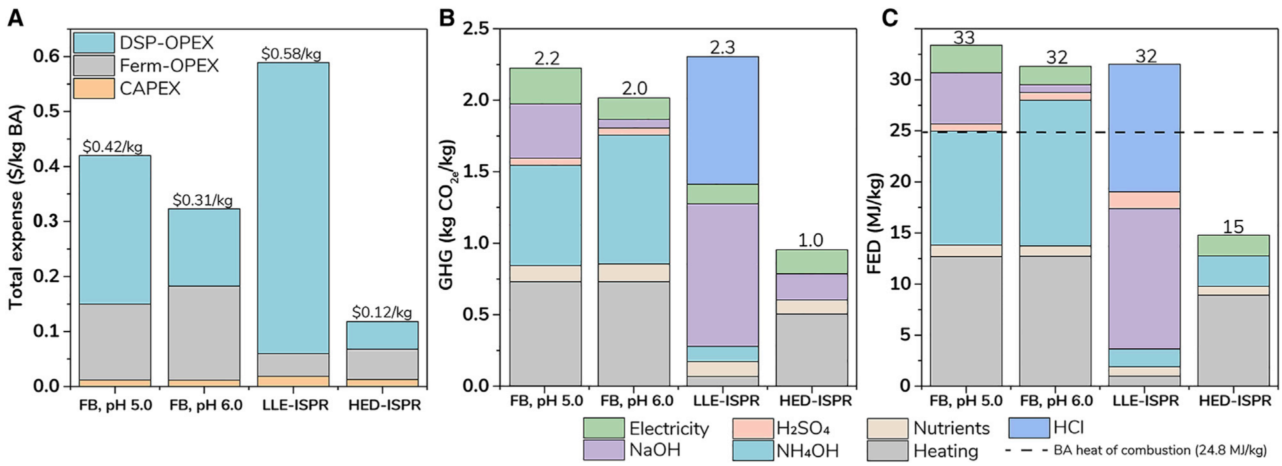

Figure 7. TEA and LCA

(A) Total expense of FB and ISPR processes in terms of $/kg of BA produced from the n^{th}-biorefinery. The summation of the OPEX, which is split between the fermentation (Ferm) and DSP expense and CAPEX is shown as the total expense. These costs do not include sugar production from lignocellulosic sugars. The total expense accounting for sugar production is $1.23, $1.14, $1.35, and $0.84/kg for the FB (pH 5), FB (pH 6), LLE-ISPR, and HED-ISPR, respectively.

(B) Greenhouse gas (GHG) emissions per kilogram of BA produced from the n^{th}-biorefinery. The combined fermentation and DSP GHG emissions is shown for the FB process at pH 5 and pH 6 and for the 2 ISPR processes.

(C) Fossil energy demand (FED) per kilogram of BA produced from the n^{th}-biorefinery. The combined fermentation and DSP FED is shown for the FB process at pH 5 and pH 6 and for the 2 ISPR processes. The heat of combustion of BA is indicated on the graph (24.8 MJ/kg) to highlight that the FB cases are both unsustainable from an energy perspective (more energy is required to generate BA than produced by the product BA if the BA is burned directly as a fuel).

Specific DSP costs (Figure S33B) are associated with either electricity, acidification, or neutralizing chemicals (H_2SO_4 and NaCl or NaOH), separation materials (membranes used in the ISPR processes or resins used in the FB DSP), and heating (for distillation or evaporation). The major unit operations for the FB, LLE-ISPR, and HED-ISPR are shown in Figures S34, S26, and S28, respectively. In all cases, there is a small electricity cost associated with pumps and motors in the process. The acid cost is due to its addition during DSP to acidify sodium butyrate produced during the process. In the FB cases, sodium butyrate in the broth is acidified using a cation exchange resin regenerated with 10 wt% H_2SO_4. The cation exchange resin was assumed to have a lifetime of 2 years, leading to the material cost shown in Figure S33B. In the LLE-ISPR process, sodium butyrate collected in the base loop is acidified with the direct addition of H_2SO_4 in a simple mixing vessel. However, for the HED-ISPR process, these large acidification expenses are circumvented. The cost of base, used for neutralization of the BA, is the highest OPEX expense for both the FB process (56% for the FB, pH 5 process) and for the LLE-ISPR process (75%). However, the NaOH cost is eliminated in the HED-ISPR process. This is because the DSP process for the HED-ISPR process does not convert BA to a carboxylate salt, as occurs in the other processes. The reduction of acidification and neutralizing chemicals is the primary reason why the DSP OPEX of the HED-ISPR process is lower than all of the other processes (2.9× lower than the FB at pH 6 process). Because the HED-ISPR uses distillation, a heating cost is added to the process, associated with the reboiler duties in the flash drum and polishing column. In addition, both ISPR processes have a material cost associated with the membrane contactors (assumed to have a lifetime of 5 years).[37] Finally, the total expense shown in Figure 7A is the summation of the CAPEX and OPEX expenses across the fermentation and DSP areas. The total process expense is $0.42, $0.31, $0.58, and $0.12/kg for the FB (pH 5), FB (pH 6), LLE-ISPR, and HED-ISPR, respectively. Lastly, the sugar feedstock production cost (Table S6), which accounts for the CAPEX and OPEX of raw material (corn stover) handling, pretreatment, and enzymatic hydrolysis, was added to the processing cost to show the cost increase associated with using a lignocellulosic biomass feedstock. The total expense accounting for sugar production is then \$1.23, \$1.14, \$1.29, and \$0.84/kg for the FB (pH 5), FB (pH 6), LLE-ISPR, and HED-ISPR, respectively. Finally, if variable OPEX and taxes are incorporated into the TEA, then the minimum product selling price (MPSP) is \$1.32, \$1.21, \$1.39, and \$0.99/kg for the FB (pH 5), FB (pH 6), LLE-ISPR, and HED-ISPR, respectively. A sensitivity analyses was also conducted to show the impact of extractant losses from the system (Figure S35; Note S7).

The GHG emissions and FED were estimated to show comparatively how effectively the HED-ISPR process lowers the environmental impact of BA production compared to the FB and LLE-ISPR case. The GHG emissions and FED of the fermentation and DSP operations were derived from the energy and material flows of each process (Table S15) (see Materials and methods). The results from the LCA are shown in Figures 7B and 7C. GHG emissions were calculated using a 100-year GHG emission factor and is calculated with units of grams of carbon dioxide equivalent (CO_{2e}).[38] FED is the energy associated with the production of raw materials or the energy used within the process (e.g., the heating FED is associated with the distillation energy requirement). In both categories of GHG emissions and FED, the NH_4OH and NaOH are the primary contributors. Ultimately, HED-ISPR shows GHG emissions and FED that are ~50% of the metrics at FB, pH 6 case. This result is mainly due to the elimination of NaOH from the HED-ISPR process and the minimum dependence on NH_4OH needed in the fermenter for pH control.

DISCUSSION

The production of fuels from biomass is critical to diminish our reliance on petroleum and build a sustainable bioeconomy.[8] Synthetic biology is a powerful approach for *de novo* production of a myriad of fuel and chemical precursors in a variety of organisms.[39,40] However, the strategy undertaken in this study was to evaluate "nature's best" microbes that are already able to produce BA from monomeric sugars, while simultaneously linking microbial performance with conditions needed for DSP development. BA is a major product in both *C. butyricum* and *C. tyrobutyricum*, but their metabolic capacities are very different (Figure 2C). These results are likely due to their intrinsic metabolic pathways; acetate is a "dead-end" carbon product in *C. butyricum,* whereas acetate is reassimilated to produce BA in *C. tyrobutyricum* (Figure 1).[15] Chain elongation of carboxylic acids via acetate reassimilation has been previously reported in other BA-producing organisms (i.e., *Clostridium kluyveri*); however, these microbes typically require ethanol as an electron donor[41] and have not been reported to use sugars as an energy source. Therefore, *C. tyrobutyricum* is an excellent microbial chassis to produce BA from lignocellulosic sugars and pursue homo-butyrate fermentations, especially at pHs ≤5 that are required for effective operation of the HED-ISPR process. Furthermore, tolerance to the end product is another important variable to select adequate biocatalysts; this study has also shown that *C. tyrobutyricum* is more tolerant to BA than *C. butyricum* (see Note S8).

Glucose and xylose co-utilization is a desired microbial feature to develop bioprocesses from lignocellulosic hydrolysates regardless of DSP operations.[42,43] Carbon catabolite repression, with preferential glucose utilization, was observed in *C. tyrobutyricum* while fermenting mixed sugars (Figure 1B).[44] Here, we have been able to cope with this diauxie via bioprocess development (Figures 5E and 5F). In contrast, arabinose accumulated in the bioreactor in ISPR setups. Arabinose utilization by *C. tyrobutyricum* has been reported to be poor, with growth lags >72 h when utilized as the sole carbon source.[45] Similarly, galactose is not efficiently utilized by *C. tyrobutyricum* either.[46] Genetic engineering has been successfully applied to this bacterial strain to enhance the utilization of these minor sugars[45,46] and will be further considered to improve the bacterial performance.

Redox and energy balances are essential for the viability of biological systems. In general, *C. tyrobutyricum* increases carbon flux toward acetate to generate higher ATP concentrations during the growth phase[12] (Figure 6). Then, BA[12] and H_2 (via ferredoxins)[47] are produced to cope with the excess of NADH and regenerate NAD^+. Apart from these general metabolic effects when fermenting sugars, here, we show that the catabolism of different sugars (glucose or xylose) greatly affects the overall bacterial performance (Figures 5 and 6), which is likely due to redox and/or energy imbalances. Xylose-containing fermentations led to acetate and formate metabolic yield decreases (close to zero), which resulted in further lactate accumulation and cells becoming inactive in their core metabolism (Figure 6). In contrast, glucose-only containing fermentations showed constant acetate and lactate metabolic yields and negligible formate formation. Acetate (mol) production per mol of xylose is lower than that per mol of glucose (1.66 and 2, respectively).[48] However, stoichiometry alone cannot explain the lower metabolic flux toward acetate in xylose-containing media compared to glucose-only-containing media over time. Overall, if acetate generation decreases, then ATP levels would also be reduced (Figure 6), which may eventually generate an energetic deficiency. It is also worth considering that pH 5 is likely not an optimal pH for *C. tyrobutyricum*, which may require additional ATP to pump protons extracellularly.[49] In addition, if acetate production ceases and it is fully reassimilated to BA, then the flux toward butyryl-CoA, which involves the utilization of 2 molecules of NADH (Figure 6), may also decrease. Therefore, lactate would be produced to regenerate NAD^+ and maintain redox balance instead. Lactate production, as a result of acetate depletion, has been previously observed when adding benzyl viologen in cultivations to increase NADH levels.[44] Thus, all of these results suggest that lactate is produced because of an excess of NADH. Ultimately, these energetic and redox events may lead to cell death and the termination of the fermentation.

Metabolic shifts have been previously reported for *C. tyrobutyricum* in xylose-containing media compared to glucose media when lowering the pH from 6 to 5.[18,50] Nevertheless, the results differed compared to the ones obtained in this study—acetate accumulated instead of being depleted from the media. The utilization of xylose and glucose potentially generates the same redox state in the cell if xylose is metabolized via the pentose phosphate pathway (Figure 6). Thus, a hypothetical cause for these differences would be the presence of a phosphoketolase pathway (from xylulose-5-phosphate to glyceraldehyde-3-phosphate and acetyl phosphate; Figure 6), which would generate a different redox state if xylose is used as a substrate.[51] The phosphoketolase pathway has not been described in *C. tyrobutyricum* yet; however, its genome encodes a putative phosphoketolase with high homology to that reported in *C. acetobutylicum*[52] (Figure S36). The presence of this pathway, which would enhance carbon conservation from xylose to acetyl phosphate and ultimately to acetate and butyrate, may be the cause of higher yields than those reported to be maximum theoretical yields from glucose (0.49 g/g[53]). Metabolic flux analysis has been conducted in *C. tyrobutyricum*, but only utilizing glucose as a substrate.[47,54,55] Therefore, further metabolic flux analysis with ^{13}C-xylose will be required to understand the basis of these metabolic differences.

C. tyrobutyricum has been exhaustively evaluated in batch and FB cultivation modes in pure sugars (i.e., glucose and less frequently xylose) and lignocellulosic substrates (e.g., corn fiber, corncob, corn husk, cane molasses, sugar cane bagasse, wheat straw).[10,14,56,57] Maximum titers and yields reported in the literature are, in general, close to 60 g/L and 0.45 g/g, similar to what we report from corn stover hydrolysate (Figure 4). In contrast, information relative to the performance of C. tyrobutyricum coupled to ISPR processes is very limited. A maximum BA titer of 300 g/L was reported in 2003 in an ISPR-based process in which BA was extracted in an organic solvent and further stripped in NaOH.[24] However, the carbon source in this fermentation was pure glucose. As far as we know, here, we report the highest BA titer from lignocellulosic substrates in an ISPR process to date (78 g/L). The titer obtained in the HED-ISPR setup from biomass hydrolysate was lower (46 g/L). Future work will focus on testing solvents with lower toxicity but with equivalent properties as those found for Cyanex 923 to increase BA production.

In regard to the economics of BA production, the HED-ISPR process has the lowest overall cost. In comparison to the FB, pH 6 case, HED-ISPR reduces the combined OPEX and CAPEX by 2.7-fold. Furthermore, when compared to the widely used state-of-the-art LLE-ISPR process (Figure 5B), HED-ISPR has a 5× lower total cost (Figure 7A). The higher cost of LLE-ISPR results from the chemical consumption of NaOH in the base loop (at least a 1:1 molar amount of NaOH to BA is needed in the base loop for effective back extraction of BA from the organic phase). During back extraction, the NaOH reacts with the BA to form sodium butyrate in an aqueous solution. As a result, acidification is then needed downstream to convert sodium butyrate to BA. Ultimately, the total expense is dramatically reduced in the HED-ISPR case because of the minimization of acid and base materials required for acidification and neutralization. The importance of removing chemical consumption from fermentation and DSP to reduce OPEX has been highlighted for other bio-based carboxylic acid production, including succinic acid production, in which 90% of OPEX was due to acid and base consumption.[27] The total HED-ISPR process cost ($0.12/kg) is only 6.7% of the total current market price of BA ($1.8/kg). However, when the cost of second-generation sugar production, variable expenses, and taxes are added to the HED-ISPR process cost, the MPSP is $0.99/kg BA. Thus, the HED-ISPR ($0.12/kg BA) expense is 12% relative to the MPSP. Typically, DSP accounts for 20%–40% of the product cost of commodity bio-based products such as ethanol and citric acid.[58] Accordingly, the HED-ISPR process for BA production from corn stover is within the industrially relevant range for commodity bio-based DSP processes. It is also worth noting that the current TEA has been conducted for a sub-optimal HED-ISPR process. For instance, we anticipate that using less-toxic organic solvents with similar properties, which would expand the fermentation length, would further improve the economics of the process. Lastly, our TEA analysis also shows that the HED-ISPR process is competitive with other developed ISPR approaches that were recently published, and information is detailed in Note S9.

In terms of the environmental impacts of BA production, the HED-ISPR process reduces both the GHG emissions and FED compared to the traditional FB process and LLE-ISPR process. GHG emissions are reduced by ~50% compared to FB and LLE-ISPR processes (Figure 7B). The reduction in GHG and FED for HED-ISPR is mostly due to the minimization of caustic chemical production. In a similar vein, recent life-cycle analysis (LCA) of the microbial production of caproic acid has pointed to a high global warming potential, acidification potential, and eutrophication potential associated with NaOH use in the DSP of that process.[59] However, the elimination of caustics is offset partially by additional heating requirements for the

HED-ISPR process compared to the traditional processes. The extra heating demand does not add a substantial energy penalty, as the total FED of HED-ISPR is less than the other processes (Figure 7C) and is only 60% of the heat of combustion of BA (24.8 MJ/kg), if the BA was used directly as a fuel. Energy efficiency within the biorefinery is known to correlate linearly to the biorefinery OPEX, and therefore minimizing energy consumption is critical to achieve industrial viability and sustainability.[60] Accordingly, a mathematical model of the HED-ISPR process has shown that the energy consumption of the HED-ISPR process can be minimized to <20% of the product heating value by loading the organic phase to higher concentrations of BA. Higher loading of BA in the organic phase results in less mass of the extractant fed to the flash distillation column, and this lowers the energy consumption. In this study, the BA concentration in the organic phase was ~4 wt%, resulting in a total energy consumption of 60% of the BA HHV. However, if the BA organic phase concentration increases to 10 wt% BA, then the distillation energy demand is reduced to 20% of the BA HHV (Figure S37). To achieve 10 wt% BA in a Cyanex 923 saturated organic phase, BA titers in the fermenter need to increase to ~30 g/L at pH 5.[22] Higher BA loading in the organic phase can be achieved by using stronger extractants that are non-toxic to the microorganisms, operating at a lower pH to generate more free BA in the fermenter, and/or increasing the tolerance to product. This increases the driving force for extraction and loads the extractant with a greater concentration of BA. Overall, here, we show a promising strategy to efficiently produce BA from lignocellulosic sugars and highlight future research areas to improve the biocatalyst and the HED-ISPR process toward the production of renewable fuels and chemicals via industrially relevant and environmentally friendly processes.

EXPERIMENTAL PROCEDURES

Resource availability

Lead contact

Further information and requests for resources and reagents should be directed to and will be fulfilled by the lead contact, Davinia Salvachúa (davinia.salvachua@nrel.gov).

Materials availability

All requests for materials should be directed to the lead contact (davinia.salvachua@nrel.gov). For plasmids, a completed materials transfer agreement may also be required.

Data and code availability

All of the experimental and computational data are available upon reasonable request to the lead contact author. This article does not report original code.

Materials and methods

See the Supplemental experimental procedures for full details.

SUPPLEMENTAL INFORMATION

Supplemental information can be found online at https://doi.org/10.1016/j.xcrp.2021.100587.

ACKNOWLEDGMENTS

This work was authored by the Alliance for Sustainable Energy, the manager and operator of the National Renewable Energy Laboratory for the U.S. Department of

Energy (DOE) under contract no. DE-AC36-08GO28308. Funding was provided by the U.S. DOE Office of Energy Efficiency and Renewable Energy and Bioenergy Technologies Office and in collaboration with the BETO Bioprocessing Separations Consortium. We thank Dan Shell and the team working in the pilot plant at the National Renewable Energy Laboratory for the generation of corn stover hydrolysates.

AUTHOR CONTRIBUTIONS

D.S., G.T.B., E.M.K., and J.G.L. provided the conceptual framework, and D.S., E.M.K., and J.G.L. directed the study. D.S., P.O.S., R.S.N., and A.M. designed and/or conducted FB and LLE-ISPR fermentations. C.S., P.O.S., and H.R.M. designed and conducted the HED-ISPR fermentations. N.S.C. built the LLE-ISPR and HED-ISPR systems. C.d.C., Y.-C.C., and M.T.G. conducted the metabolic engineering work. P.O.S., I.M., and E.C.D.T. conducted the TEA and LCA analyses. D.J.P. and S.H. conducted the analytical work. D.S. and P.O.S. drafted the initial manuscript, followed by editing and interpretation from all of the co-authors.

DECLARATION OF INTERESTS

The authors declare no competing interests. P.S. and E.M.K. have a patent related to this work submitted by the Alliance for Sustainable Energy on Advanced Anaerobic Digestion to Carboxylic Acids (US patent application no. 17/306,251, filed on May 3, 2021). G.T.B. is a board member of *Cell Reports Physical Science*.

INCLUSION AND DIVERSITY

One or more of the authors of this paper self-identifies as an underrepresented ethnic minority in science.

Received: May 14, 2021
Revised: July 26, 2021
Accepted: September 1, 2021
Published: October 11, 2021

REFERENCES

1. Pacala, S., and Socolow, R. (2004). Stabilization wedges: solving the climate problem for the next 50 years with current technologies. Science *305*, 968–972.

2. Rogers, J.N., Stokes, B., Dunn, J., Cai, H., Wu, M., Haq, Z., and Baumes, H. (2017). An assessment of the potential products and economic and environmental impacts resulting from a billion ton bioeconomy. Biofuels Bioprod. Biorefin. *11*, 110–128.

3. Serrano-Ruiz, J.C., and Dumesic, J.A. (2011). Catalytic routes for the conversion of biomass into liquid hydrocarbon transportation fuels. Energy Environ. Sci. *4*, 83–99.

4. Shylesh, S., Gokhale, A.A., Ho, C.R., and Bell, A.T. (2017). Novel strategies for the production of fuels, lubricants, and chemicals from biomass. Acc. Chem. Res. *50*, 2589–2597.

5. Jamalzade, E., Kashkooli, K., Griffin, L., van Walsum, G.P., and Schwartz, T.J. (2021). Production of jet-fuel-range molecules from biomass-derived mixed acids. React. Chem. Eng. *6*, 845.

6. Rozmysłowicz, B., Yeap, J.H., Elkhaiary, A.M.I., Talebi Amiri, M., Shahab, R.L., Questell-Santiago, Y.M., Xiros, C., Le Monnier, B.P., Studer, M.H., and Luterbacher, J.S. (2019). Catalytic valorization of the acetate fraction of biomass to aromatics and its integration into the carboxylate platform. Green Chem. *21*, 2801–2809.

7. Huq, N.A., Hafenstine, G.R., Huo, X., Nguyen, H., Tifft, S.M., Conklin, D.R., Stück, D., Stunkel, J., Yang, Z., Heyne, J.S., et al. (2021). Toward net-zero sustainable aviation fuel with wet waste-derived volatile fatty acids. Proc. Natl. Acad. Sci. USA *118*, e2023008118.

8. Huo, X., Huq, N.A., Stunkel, J., Cleveland, N.S., Starace, A.K., Settle, A.E., York, A.M., Nelson, R.S., Brandner, D.G., Fouts, L., et al. (2019). Tailoring diesel bioblendstock from integrated catalytic upgrading of carboxylic acids: a "fuel property first" approach. Green Chem. *21*, 5813–5827.

9. Kwon, O., and Han, J. (2021). Supply chain management of butyric acid-derived butanol: Stochastic approach. Appl. Energy *297*, 117119.

10. Jiang, L., Fu, H., Yang, H.K., Xu, W., Wang, J., and Yang, S.T. (2018). Butyric acid: applications and recent advances in its bioproduction. Biotechnol. Adv. *36*, 2101–2117.

11. Holtzapple, M.T., and Granda, C.B. (2009). Carboxylate platform: the MixAlco process part 1: comparison of three biomass conversion platforms. Appl. Biochem. Biotechnol. *156*, 95–106.

12. Yang, S.T., Yu, M., Chang, W.L., and Tang, I.C. (2013). Anaerobic fermentations for the production of acetic and butyric acids. In Bioprocessing Technologies in Biorefinery for Sustainable Production of Fuels, Chemicals, and Polymers, H.A.E.-E. Shang-Tian Yang, ed. (Nuttha Thongchul), pp. 351–374.

13. Dwidar, M., Park, J.Y., Mitchell, R.J., and Sang, B.I. (2012). The future of butyric acid in industry. ScientificWorldJournal *2012*, 471417.

14. Huang, J., Tang, W., Zhu, S., and Du, M. (2018). Biosynthesis of butyric acid by *Clostridium tyrobutyricum*. Prep. Biochem. Biotechnol. *48*, 427–434.

15. Lee, J., Jang, Y.S., Han, M.J., Kim, J.Y., and Lee, S.Y. (2016). Deciphering *Clostridium*

tyrobutyricum metabolism based on the whole-genome sequence and proteome analyses. MBio *7*, e00743-16.

16. Yu, M., Zhang, Y., Tang, I.C., and Yang, S.-T. (2011). Metabolic engineering of *Clostridium tyrobutyricum* for n-butanol production. Metab. Eng. *13*, 373–382.

17. Liu, X., Zhu, Y., and Yang, S.-T. (2006). Butyric acid and hydrogen production by *Clostridium tyrobutyricum* ATCC 25755 and mutants. Enzyme Microb. Technol. *38*, 521–528.

18. Zhu, Y., and Yang, S.-T. (2004). Effect of pH on metabolic pathway shift in fermentation of xylose by *Clostridium tyrobutyricum*. J. Biotechnol. *110*, 143–157.

19. Jarboe, L.R., Royce, L.A., and Liu, P. (2013). Understanding biocatalyst inhibition by carboxylic acids. Front. Microbiol. *4*, 272.

20. Du, J., McGraw, A., Lorenz, N., Beitle, R.R., Clausen, E.C., and Hestekin, J.A. (2012). Continuous fermentation of *Clostridium tyrobutyricum* with partial cell recycle as a long-term strategy for butyric acid production. Energies *5*, 2835–2848.

21. Michel-Savin, D., Marchal, R., and Vandecasteele, J.P. (1990). Butyrate production in continuous culture of *Clostridium tyrobutyricum*: effect of end-product inhibition. Appl. Microbiol. Biotechnol. *33*, 127–131.

22. Saboe, P.O., Manker, L.P., Michener, W.E., Peterson, D.J., Brandner, D.G., Deutch, S.P., Kumar, M., Cywar, R.M., Beckham, G.T., and Karp, E.M. (2018). *In situ* recovery of bio-based carboxylic acids. Green Chem. *20*, 1791–1804.

23. Zigová, J., Šturdík, E., Vandák, D., and Schlosser, Š. (1999). Butyric acid production by *Clostridium butyricum* with integrated extraction and pertraction. Process Biochem. *34*, 835–843.

24. Wu, Z., and Yang, S.T. (2003). Extractive fermentation for butyric acid production from glucose by *Clostridium tyrobutyricum*. Biotechnol. Bioeng. *82*, 93–102.

25. Nuchnoi, P., Izawa, I., Nishio, N., and Nagai, S. (1987). Extractive acidogenic fermentation by a supported liquid membrane. J. Ferment. Technol. *65*, 699–702.

26. Nelson, R.S., Peterson, D.J., Karp, E.M., Beckham, G.T., and Salvachúa, D. (2017). Mixed carboxylic acid production by *Megasphaera elsdenii* from glucose and lignocellulosic hydrolysate. Fermentation (Basel) *3*, 10.

27. Biddy, M.J., Davis, R., Humbird, D., Tao, L., Dowe, N., Guarnieri, M.T., Linger, J.G., Karp, E.M., Salvachúa, D., Vardon, D.R., and Beckham, G.T. (2016). The techno-economic basis for coproduct manufacturing to enable hydrocarbon fuel production from lignocellulosic biomass. ACS Sustain. Chem. Eng. *4*, 3196–3211.

28. Saboe, P.O., Monroe, H.R., Michener, W.E., Manker, L.P., Haugen, S.J., Beckham, G.T., and Karp, E.M. (2019). In situ product recovery of bio-based ethyl esters via hybrid extraction-distillation. Green Chem. *21*, 5306–5315.

29. Sheng, C., and Azevedo, J.L.T. (2005). Estimating the higher heating value of biomass fuels from basic analysis data. Biomass Bioenergy *28*, 499–507.

30. Carstensen, F., Apel, A., and Wessling, M. (2012). In situ product recovery: submerged membranes vs. external loop membranes. J. Membr. Sci. *394-395*, 1–36.

31. Jaffrin, M.Y. (2008). Dynamic shear-enhanced membrane filtration: a review of rotating disks, rotating membranes and vibrating systems. J. Membr. Sci. *324*, 7–25.

32. Zsirai, T., Qiblawey, H., A-Marri, M.J., and Judd, S. (2016). The impact of mechanical shear on membrane flux and energy demand. J. Membr. Sci. *516*, 56–63.

33. He, G.Q., Kong, Q., Chen, Q.H., and Ruan, H. (2005). Batch and fed-batch production of butyric acid by *clostridium butyricum* ZJUCB. J. Zhejiang Univ. Sci. B *6*, 1076–1080.

34. Straathof, A.J.J. (2014). Transformation of biomass into commodity chemicals using enzymes or cells. Chem. Rev. *114*, 1871–1908.

35. Huq, N.A., Huo, X., Hafenstine, G.R., Tifft, S.M., Stunkel, J., Christensen, E.D., Fioroni, G.M., Fouts, L., McCormick, R.L., Cherry, P.A., et al. (2019). Performance-advantaged ether diesel bioblendstock production by a priori design. Proc. Natl. Acad. Sci. USA *116*, 26421.

36. Tan, E.C.D., Snowden-Swan, L.J., Talmadge, M., Dutta, A., Jones, S., Ramasamy, K.K., Gray, M., Dagle, R., Padmaperuma, A., Gerber, M., et al. (2017). Comparative techno-economic analysis and process design for indirect liquefaction pathways to distillate-range fuels via biomass-derived oxygenated intermediates upgrading. Biofuels Bioprod. Biorefin. *11*, 41–66.

37. Cote, P., Alam, Z., and Penny, J. (2012). Hollow fiber membrane life in membrane bioreactors (MBR). Desalination *288*, 145–151.

38. Stocker, T.F., Qin, D., Plattner, G.-K., Tignor, M., Allen, S.K., Boschung, J., Nauels, A., Xia, Y., Bex, V., and Midgley, P.M. (2013). In Climate Change 2013: The Physical Science Basis. Contribution of Working Group I to the Fifth Assessment Report of the Intergovernmental Panel on Climate Change, T.F. Stocker, D. Qin, G.-K. Plattner, M.M.B. Tignor, S.K. Allen, J. Boschung, A. Nauels, Y. Xia, V. Bex, P.M. Midgley, and Working Group I Technical Support Unit., eds. (Cambridge University Press), p. 1535.

39. Lee, S.Y., Kim, H.U., Chae, T.U., Cho, J.S., Kim, J.W., Shin, J.H., Kim, D.I., Ko, Y.-S., Jang, W.D., and Jang, Y.-S. (2019). A comprehensive metabolic map for production of bio-based chemicals. Nat. Catal. *2*, 18–33.

40. Shanks, B.H., and Keeling, P.L. (2017). Bioprivileged molecules: creating value from biomass. Green Chem. *19*, 3177–3185.

41. Angenent, L.T., Richter, H., Buckel, W., Spirito, C.M., Steinbusch, K.J.J., Plugge, C.M., Strik, D.P.B.T.B., Grootscholten, T.I.M., Buisman, C.J.N., and Hamelers, H.V.M. (2016). Chain elongation with reactor microbiomes: open-culture biotechnology to produce biochemicals. Environ. Sci. Technol. *50*, 2796–2810.

42. Garcia Sanchez, R., Karhumaa, K., Fonseca, C., Sànchez Nogué, V., Almeida, J.R.M., Larsson, C.U., Bengtsson, O., Bettiga, M., Hahn-Hägerdal, B., and Gorwa-Grauslund, M.F. (2010). Improved xylose and arabinose utilization by an industrial recombinant *Saccharomyces cerevisiae* strain using evolutionary engineering. Biotechnol. Biofuels *3*, 13.

43. Sànchez Nogué, V., and Karhumaa, K. (2015). Xylose fermentation as a challenge for commercialization of lignocellulosic fuels and chemicals. Biotechnol. Lett. *37*, 761–772.

44. Fu, H., Yu, L., Lin, M., Wang, J., Xiu, Z., and Yang, S.T. (2017). Metabolic engineering of *Clostridium tyrobutyricum* for enhanced butyric acid production from glucose and xylose. Metab. Eng. *40*, 50–58.

45. Chen, T., Zhang, L., Luo, G., and Yuan, W. (2017). Butyric acid production by *Clostridium tyrobutyricum* in sugar mixtures and corncob hydrolysate containing arabinose. BioResources *12*, 7931–7942.

46. He, F., Qin, S., Yang, Z., Bai, X., Suo, Y., and Wang, J. (2020). Butyric acid production from spent coffee grounds by engineered *Clostridium tyrobutyricum* overexpressing galactose catabolism genes. Bioresour. Technol. *304*, 122977.

47. Jiang, L., Song, P., Zhu, L., Li, S., Hu, Y., Fu, N., and Huang, H. (2013). Comparison of metabolic pathway for hydrogen production in wild-type and mutant *Clostridium tyrobutyricum* strain based on metabolic flux analysis. Int. J. Hydrogen Energy *38*, 2176–2184.

48. Reginatto, V., and Antônio, R.V. (2015). Fermentative hydrogen production from agroindustrial lignocellulosic substrates. Braz. J. Microbiol. *46*, 323–335.

49. Ciranna, A., Pawar, S.S., Santala, V., Karp, M., and van Niel, E.W.J. (2014). Assessment of metabolic flux distribution in the thermophilic hydrogen producer *Caloramator celer* as affected by external pH and hydrogen partial pressure. Microb. Cell Fact. *13*, 48.

50. Liu, X., Zhu, Y., and Yang, S.T. (2006). Construction and characterization of ack deleted mutant of *Clostridium tyrobutyricum* for enhanced butyric acid and hydrogen production. Biotechnol. Prog. *22*, 1265–1275.

51. Servinsky, M.D., Germane, K.L., Liu, S., Kiel, J.T., Clark, A.M., Shankar, J., and Sund, C.J. (2012). Arabinose is metabolized via a phosphoketolase pathway in *Clostridium acetobutylicum* ATCC 824. J. Ind. Microbiol. Biotechnol. *39*, 1859–1867.

52. Liu, L., Zhang, L., Tang, W., Gu, Y., Hua, Q., Yang, S., Jiang, W., and Yang, C. (2012). Phosphoketolase pathway for xylose catabolism in *Clostridium acetobutylicum* revealed by ^{13}C metabolic flux analysis. J. Bacteriol. *194*, 5413–5422.

53. Luo, H., Yang, R., Zhao, Y., Wang, Z., Liu, Z., Huang, M., and Zeng, Q. (2018). Recent advances and strategies in process and strain engineering for the production of butyric acid by microbial fermentation. Bioresour. Technol. *253*, 343–354.

54. Jo, J.H., and Kim, W. (2016). Carbon material distribution and flux analysis under varying glucose concentrations in hydrogen-

producing *Clostridium tyrobutyricum* JM1. J. Biotechnol. *228*, 103–111.

55. Cheng, H.-H., Whang, L.-M., Lin, C.-A., Liu, I.C., and Wu, C.-W. (2013). Metabolic flux network analysis of fermentative hydrogen production: using *Clostridium tyrobutyricum* as an example. Bioresour. Technol. *141*, 233–239.

56. Maiti, S., Brar, S.K., Verma, M., Soccol, C.R., and Maiti, D.C. (2016). Butyric acid: a platform chemical for biofuel and high-value biochemicals. In Platform Chemical Biorefinery, S. Kaur Brar, S. Jyoti Sarma, and K. Pakshirajan, eds. (Elsevier), pp. 119–132.

57. Xiao, Z., Cheng, C., Bao, T., Liu, L., Wang, B., Tao, W., Pei, X., Yang, S.-T., and Wang, M. (2018). Production of butyric acid from acid hydrolysate of corn husk in fermentation by *Clostridium tyrobutyricum*: kinetics and process economic analysis. Biotechnol. Biofuels *11*, 164.

58. Straathof, A. (2011). The proportion of downstream costs in fermentative production processes. In Comprehensive Biotechnology, *Volume 2*, M. Moo-Young, ed. (Elsevier), pp. 811–814.

59. Chen, W.S., Strik, D.P.B.T.B., Buisman, C.J.N., and Kroeze, C. (2017). Production of caproic acid from mixed organic waste: an environmental life cycle perspective. Environ. Sci. Technol. *51*, 7159–7168.

60. Lange, J.P. (2007). Lignocellulose conversion: an introduction to chemistry, process and economics. Biofuels Bioprod. Biorefin. *1*, 39–48.